Available online at www.sciencedirect.com
SCIENCE DIRECT®
Bioorganic & Medicinal Chemistry 13 (2005) 47–57
Bioorganic & Medicinal Chemistry

Photocontrol of nitric oxide production in cell culture using a caged isoform selective inhibitor

Basil Perdicakis,[a,†] Heather J. Montgomery,[b,†] Glenn L. Abbott,[b] Dan Fishlock,[b] Gilles A. Lajoie,[c] J. Guy Guillemette[b] and Eric Jervis[a,*]

[a]*Department of Chemical Engineering, University of Waterloo, Waterloo, ON, Canada N2L 3G1*
[b]*Department of Chemistry, University of Waterloo, Waterloo, ON, Canada N2L 3G1*
[c]*Department of Biochemistry, University of Western Ontario, London, ON, Canada N6A 5C1*

Received 17 June 2004; revised 3 October 2004; accepted 4 October 2004
Available online 2 November 2004

Abstract—Over the past decade, multiphoton microscopy has progressed from a photonic novelty to a technique whose application is currently experiencing exponential growth in the biological sciences. A novel application of this technology with significant therapeutic potential is the control of drug activity by multiphoton photolysis of caged therapeutics. As an initial case study, the potent isoform selective inhibitor N-(3-(aminomethyl)benzyl) acetamidine (1400W) of inducible nitric oxide synthase (iNOS) has been conjugated to a caging molecule 6-bromo-7-hydroxy-4-hydroxyquinoline-2-ylmethyl acetyl ester (Bhc). Here we present the first report of a bulk therapeutic effect, inhibition of nitric oxide production, in mammalian cell culture by multiphoton photolysis of a caged drug, Bhc-1400W. Mouse macrophage RAW 264.7 cells induced with bacterial lipopolysaccharides to express iNOS were used to assess the therapeutic value of the conjugated inhibitor. Both 1400W and Bhc-1400W are stable in metabolically active cells and an optimal time interval for the photorelease of the inhibitor was determined. The ratios of the IC_{50} values of Bhc-1400W over 1400W calculated in the presence of iNOS enzyme and in RAW 264.7 cell culture are 19 and 100, respectively, indicating that a broad therapeutic range exists in cell culture. Multiphoton uncaging protocols and therapeutic doses of inhibitors were not cytotoxic. Photocontrol of LPS induced nitric oxide production was achieved in mammalian cell culture using a single laser focal volume. This technology has the potential to control active drug concentrations in vivo, a lack of which is one of the main problems currently associated with systemic drug administration.

1. Introduction

The critically important and diverse roles of nitric oxide (·NO) in physiology and pathology make it a desirable, but challenging molecule to control through therapeutic intervention. Three distinct isoforms of the enzyme nitric oxide synthase (NOS) catalyze the oxidation of L-arginine to ·NO in mammalian systems.[1] ·NO produced from the two constitutively expressed isoforms, neuronal NOS (nNOS) and endothelial NOS (eNOS), is regulated by the Ca^{2+}-dependent binding of calmodulin (CaM) and acts as a secondary signaling molecule.[2–4] At picomolar concentrations, nitric oxide produced by eNOS and nNOS acts as a second messenger, reversibly binding to the heme groups of proteins to signal vasodilation, relaxation of smooth muscles, and angiogenesis.[2,3] The third NOS isoform, inducible NOS (iNOS) is most commonly regulated at the transcriptional level by induction with a variety of pro-inflammatory mediators. Micromolar concentrations of ·NO produced by iNOS results in the reversible S-nitrosation of thiol groups leading to nitrosative stress. High concentrations of ·NO in the presence of oxygen or the superoxide anion (O_2^-) leads to the formation of other reactive nitrogen oxide intermediates that cause irreversible damage to proteins, nucleic acids, and other macromolecules in the cell.[5,6] ·NO production from iNOS plays important roles in the immune response, including antimicrobial, anti-tumor, and signaling functions.[7]

·NO is implicated in the pathology of numerous human diseases including cancer,[7] diabetes,[8] stroke,[9] arthritis,[10] and septic shock.[11] However, ·NO both exacerbates and

Keywords: Multiphoton; Uncaging; Nitric oxide; Drug delivery.
* Corresponding author. Tel.: +1 519 888 4567x3928; fax: +1 519 746 4979; e-mail: ericjj@cape.uwaterloo.ca
† These authors contributed equally to the research.

0968-0896/$ - see front matter © 2004 Elsevier Ltd. All rights reserved.
doi:10.1016/j.bmc.2004.10.002

reduces local tissue damage in several pathophysiological conditions.[3,7] Whether the result of ·NO production is beneficial or detrimental is usually dependent on the NOS isoform producing ·NO and the stage of the disease state. The expression of iNOS in various cells and tissues is detrimental in numerous pathological conditions. The overproduction of ·NO from iNOS has been implicated in the destruction of β-islet cells in type I diabetes, the increase in infarct volume after cerebral ischemia, the destruction of tissue in rheumatoid arthritis, and the dysfunction of organs in septic shock.[11] iNOS knockout mice have reduced infarct volumes following surgically induced focal ischemia.[12] In contrast to the damage caused by iNOS activity, eNOS activity in adjacent cells has shown therapeutic properties, relaxing vascular tissue, preventing platelet cell adhesion, and increasing blood flow to the site of injury.[4] eNOS knockout mice exhibit larger infarct volumes following induction of focal ischemia.[12] In surgically induced cerebral ischemia, ·NO production from eNOS and iNOS is most pronounced within 2 h and between 12 h and 7 days of the ischemic insult, respectively.[12]

The complex roles that ·NO plays in pathological conditions have hampered the use of generic NOS inhibitors in the treatment of these diseases. In fact, the use of the nonselective NOS inhibitor N^G-monomethyl-L-arginine (L-NMMA) to treat septic shock in humans caused adverse effects as the inhibition of eNOS led to vasoconstriction and organ ischemia.[13,14] The use of selective iNOS inhibitors has the potential to alleviate the serious side effects from the global inhibition of NOS. However, even the global inhibition of iNOS is believed to be detrimental to the health of patients.[3] For example, evidence of constitutive expression of iNOS in the human retina,[15] cerebellum, skeletal muscle,[16] and lungs[17] have been reported. Due to the diverse roles of iNOS, nNOS, and eNOS in disease and physiology, a clear need for isoform selective NOS inhibitors that can be spatially and temporally controlled is evident.[3,4]

A novel method of controlling drug delivery is to inactivate a drug by conjugation with a photolabile-protecting group (caging). After administration of the caged compound, the drug can be released, or uncaged, from the protecting group by irradiation with light. Application of this technology should only be limited by the photoaccessibility and pharmacokinetics of the target tissue. The use of high repetition mode-locked lasers to effect multiphoton (MP) photolysis of caged therapeutics using near infrared (NIR) light confers significant advantages over the use of conventional UV or short wave visible radiation to uncage molecules including reduced tissue photodamage,[18] improved tissue penetration depths,[19] and intrinsic spatial confinement of photolysis.[20,21]

In a previous report, multiphoton photorelease of the iNOS selective inhibitor 1400W[22] from the MP photolabile-protecting group, N-(6-bromo-7-hydroxycoumarin-4-ylmethyl) alcohol (Bhc),[23] was demonstrated in solution.[24] The inhibitor 1400W was one of the first potent, isoform selective inhibitors of NOS developed.[22] Coupling of 1400W to Bhc produced the photolabile compound Bhc-1400W.[24] The large two-photon action cross section of Bhc[23] allowed for the efficient photorelease of the inhibitor 1400W. Studies with purified iNOS and 1400W, UV uncaged Bhc-1400W, and multiphoton uncaged Bhc-1400W confirmed the release of 1400W from Bhc, and subsequent iNOS inhibition.[24] Similar studies with the caged compound Bhc-1400W confirmed that it does not significantly inhibit iNOS activity. These results established a large therapeutic range over which the photorelease of 1400W could be exploited.

Here we demonstrate MP uncaging of Bhc-1400W in mammalian cell culture and subsequent attenuation of ·NO production. Bhc-1400W was uncaged on the stage of a multiphoton laser scanning microscopy (MPLSM) system using parked and rastered laser beams. The stability of Bhc-1400W in cell culture was confirmed, prodrug toxicity and phototoxicity were assessed, and an optimal window for the photorelease of 1400W was determined. A broad therapeutic range was established over which the photorelease of 1400W could be exploited. Uncaging parameters were established to effectively photorelease a therapeutic concentration of 1400W from the caged compound without affecting cell viability. Bhc-1400W was uncaged in the presence of cells and shown to inhibit ·NO production without adversely affecting cellular viability. The safe and effective use of MP excitation to photorelease 1400W from Bhc-1400W in mammalian cell culture supports the use of this novel drug targeting strategy to temporally and spatially control the activation of a drug in vivo.

2. Results

2.1. Multiphoton uncaging of Bhc-1400W

Multiphoton uncaging of Bhc-1400W on the microscope stage of a MPLSM system was performed using a scanned (rastered) laser beam or with a stationary (parked) laser beam (Fig. 1). The purpose of this experiment was to confirm that Bhc-1400W could be uncaged on the microscope stage of a MPSLM system, as opposed to the laser exit,[24] and that rastering of the laser focal volume would improve the bulk uncaging efficiency. The oxyhemoglobin assay was used to assess uncaging by monitoring ·NO production from iNOS.[24] The calculated IC_{50} values (i.e., the inhibitor concentration that effects a 50% reduction in the uninhibited enzyme activity) for Bhc-1400W and UV uncaged Bhc-1400W were 344 ± 50 and 20 ± 3 nM, respectively. Coupling of Bhc to 1400W results in a significant reduction in inhibitory potency. The full inhibitory potency and NOS isoform selectivity of 1400W are regained upon complete uncaging of Bhc-1400W by either single (UV) or multiphoton (NIR) absorption.[24] The ratio of the IC_{50} value for Bhc-1400W over 1400W is 19, in good agreement with the value of 16 reported previously for the iNOS system.[24]

The decrease in IC_{50} value with increasing uncaging time, as increasing amounts of 1400W are photo-

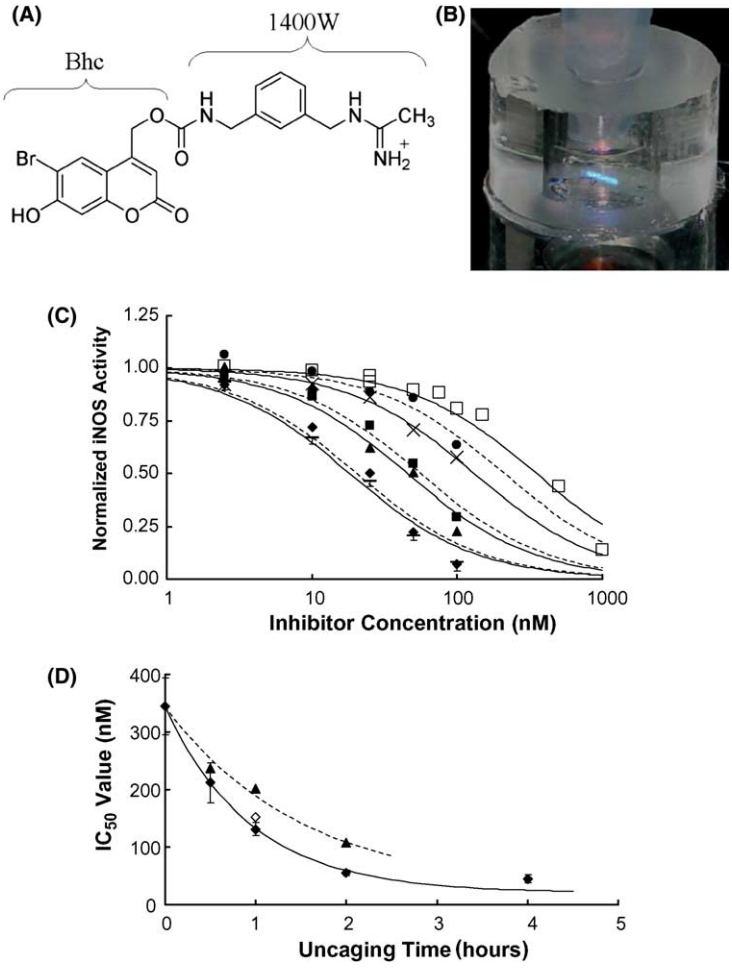

Figure 1. Multiphoton uncaging kinetics on the microscope stage of a MPLSM system. *Panel A*: expected ionic form of Bhc-1400W at pH 7.2. *Panel B*: multiphoton uncaging of Bhc-1400W on the stage of a MPLSM system using a scanned laser beam. The blue fluorescence resulting from a line scan approximately 1.5 mm in length in a concentrated Bhc-1400W solution is shown. Absorbance of the NIR laser at the top of the microcuvette appears as a reddish hue. *Panel C*: the IC_{50} values for 1400W (-,-, 18 ± 2 nM), UV uncaged Bhc-1400W (◆, -- 20 ± 3 nM), Bhc-1400W (□,–, 344 ± 49 nM), and Bhc-1400W uncaged using a rastered laser for 0.5 (●, --, 212 ± 35 nM), 1 (×,–, 131 ± 11 nM), 2 (■,--, 51 ± 5 nM), and 4 h (▲,–, 45 ± 7 nM) were determined. Similar data was obtained for Bhc-1400W MP uncaged using a parked laser beam. Error bars indicate ± 1 standard deviation and are representative of collected data. *Panel D*: IC_{50} versus uncaging time data using a parked (▲,--, first-order rate constant = 0.66 ± 0.06 h^{-1}) and rastered laser (◆,–, first-order rate constant = 1.06 ± 0.07 h^{-1}) were fit to a decaying exponential. A 1 h MP uncaged data point using a rastered laser was repeated (◊) during the day when MP uncaging data using a parked laser was obtained. All enzyme assays were performed using purified recombinant human iNOS. Errors bars denote standard errors.

released, is clearly evident from the data shown in Figure 1. The percent change in the IC_{50} value of the Bhc-1400W sample exposed to 4 h of MP uncaging using a rastered laser beam was 92%. From this data it was estimated that approximately 50% of the 10 μL volume of caged inhibitor was photoreleased. IC_{50} data for control samples were superimposable with the Bhc-1400W data shown in panel C of Figure 1.

IC_{50} versus uncaging time data was fit to a decaying exponential by nonlinear regression (Fig. 1, panel D). The regressed apparent first-order rate constants for MP uncaging of Bhc-1400W using a parked and rastered laser were 0.66 ± 0.06 h^{-1} and 1.06 ± 0.07 h^{-1}, and were significantly different at the 5% significance level (*P* value of 9×10^{-4}). A 1 h MP uncaging sample using a rastered laser (Fig. 1, panel D, Δ) was repeated on the day when uncaging data was collected using a parked laser. The IC_{50} value calculated from this data point was significantly different from the regressed IC_{50} value when a parked laser was used to uncage Bhc-1400W, but was not significantly different from the IC_{50} value calculated for the previously determined IC_{50} value following 1 h of uncaging using a rastered laser.

As expected the apparent first-order rate constants indicate that rastering significantly improves the overall uncaging efficiency. This occurs because the uncaging reaction rate at the laser focal point is much faster than the diffusion rate of Bhc-1400W back into the two-photon excitation volume. The characteristic two-photon uncaging and diffusive recovery times for the data shown in Figure 1 using a parked laser beam are on the order of microseconds and milliseconds,

respectively.[25] The mass transfer limitations that reduce the bulk uncaging efficiency using a parked laser are partially offset using a rastered laser volume where the focal volume is moved every 7 μs (Fig. 1). Experimental data are in excellent agreement with reaction–diffusion models of the MP uncaging process (data not shown). It should be noted that the apparent first-order rate constants do not have any physical meaning, but were merely used to compare the relative rates of bulk uncaging that occurred using a stationary and scanned laser beam.[26] No uncaging was observed when a Bhc-1400W sample was irradiated for 1.5 h with a NIR laser beam at 750 nm that was not mode locked.

2.2. Stability and inhibition kinetics of compounds in cell culture

The Griess assay,[27] which measures the concentration of nitrite, a stable decomposition product of ·NO in cell culture,[28] was used to detect ·NO production[29,30] from a murine macrophage cell line (RAW 264.7).[31] 1400W, UV uncaged Bhc-1400W, and Bhc-1400W (all at a concentration of 10 or 2 μM) were added to lipopolysaccharide (LPS) induced RAW 264.7 cells, and incubated for 8, 12, 16, 20, or 24 h before the Griess assay was performed. Figure 2 shows the amount of nitrite produced by the cells in the presence of inhibitor compared to no inhibitor (grey bars) for the different incubation times. Both 1400W and UV uncaged Bhc-1400W significantly inhibited nitrite production from the RAW 264.7 cells, even at the lower concentration of inhibitor (2 μM). In contrast, the caged Bhc-1400W inhibitor did not inhibit nitrite production (Fig. 2, horizontal and diagonal stripes respectively). This is not surprising since Bhc-1400W is not readily transported into cells, as evidenced by HPLC and MPLSM imaging (data not shown), and is a poor inhibitor of iNOS compared to 1400W or UV uncaged 1400W.[24] The data in Figure 2 also indicates that 1400W and uncaged Bhc-1400W are stable in cell culture over 24 h as no decrease in the inhibition of nitrite production between time points was observed for these inhibitors. Furthermore, no dark uncaging of Bhc-1400W occurred in cell culture as no increase in inhibition occurred over 24 h. Bhc-1400W incubated with cells for 3 days, and subsequently uncaged possessed a similar degree of inhibitory potency as freshly solubilized Bhc-1400W.

2.3. Optimization of inhibitor addition to cell culture

The expression of iNOS in macrophage RAW 264.7 cells occurs between 6 and 12 h after addition of an immunostimulant.[7,32] The administration of a potent iNOS inhibitor some time between the addition of an immunostimulant and the start of iNOS expression should therefore suppress nitrite production. The suppression of nitrite production will only occur as long as the inhibitor is taken up into the cells, but not readily converted to an inactive molecule or actively transported out of the cells. The potent iNOS selective inhibitor 1400W is readily taken up by cells and inhibits nitrite production, even when administered 2 h before the addition of LPS to RAW 264.7 cells (Fig. 3). Furthermore, the addition of 1400W (10 or 2 μM) to RAW 264.7 cells that had been incubating with LPS for up to 8 h caused a significant decrease in the amount of nitrite produced by these cells (Fig. 3). Significant increases in nitrite concentrations were found when 1400W was administered 10 and 20 h after induction. Overall, there is a time window of 6–8 h during which 1400W can be administered to RAW 264.7 cells, or during which Bhc-1400W may be uncaged by MPLSM, without an observable decrease in inhibitory potency.

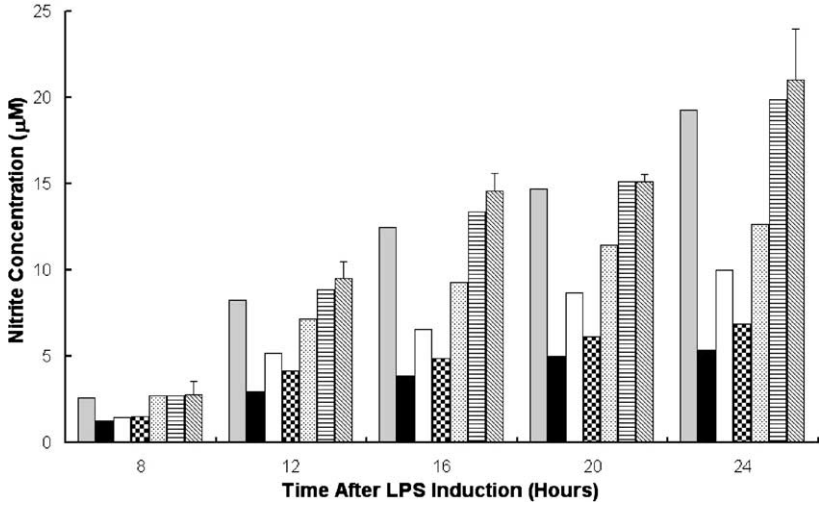

Figure 2. Time course of the ability of 1400W, UV uncaged Bhc-1400W, and Bhc-1400W to inhibit nitrite production from LPS-induced macrophage RAW 264.7 cells. The inhibitors 1400W (10 μM (black bars) and 2 μM (white bars)), UV uncaged Bhc-1400W (10 μM (checkered pattern bars) and 2 μM (dotted bars)), and Bhc-1400W (10 μM (horizontal striped bars) and 2 μM (diagonal striped bars)) were added to the LPS-induced cells (1 μg/mL, grey bars). At time intervals of 8, 12, 16, 20, and 24 h after LPS addition, the amount of nitrite present in the samples was determined by the Griess assay. Total nitrite production from control wells of cells with LPS was 20 μM. Error bars indicate 1 standard deviation and are representative of collected data.

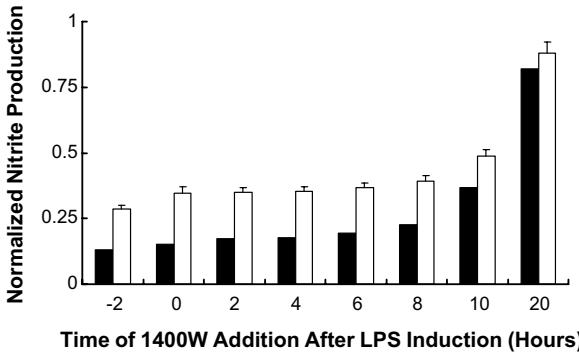

Figure 3. Optimization of 1400W addition to LPS-induced RAW 264.7 cells. Different concentrations of 1400W, 10 μM (black bars) or 2 μM (white bars), were added to RAW 264.7 cells at different time periods before and after LPS induction (1 μg/mL) in order to determine the optimum time for addition of the inhibitor. The inhibitor 1400W was added at different times, 2 h before, or at 0, 2, 4, 6, 8, 10, and 20 h after LPS induction. After 24 h incubation with LPS the Griess assay was used to determine the amount of nitrite produced. Total nitrite production from control wells of cells with LPS was 14 μM. Error bars indicate 1 standard deviation and are representative of collected data.

2.4. Inhibition of ·NO production in mammalian cell culture

The inhibitory potency of 1400W, uncaged Bhc-1400W, Bhc-1400W, Bhc, and UV irradiated Bhc against nitrite production in LPS-stimulated RAW 264.7 cells were assessed. IC_{50} curves (Fig. 4) were obtained by normalizing nitrite production from LPS-induced RAW 264.7 cells incubated for 24 h with varying amounts of inhibitor against LPS-induced cells incubated in the absence of inhibitor. IC_{50} values (i.e., the inhibitor concentration that effects a 50% reduction in nitrite production from LPS-stimulated cells) characterizing the inhibition of ·NO production were calculated.[24] The IC_{50} values for UV uncaged Bhc-1400W (IC_{50} value of 2.6 ± 0.1 μM) and MP uncaged Bhc-1400W (IC_{50} values of 4.2 ± 0.8 and 4.8 ± 0.3 μM for MP uncaging at the laser exit and on the microscope stage, respectively) indicate that uncaged Bhc-1400W exhibits similar efficacy in cell culture studies as the iNOS inhibitor 1400W (IC_{50} value of 2.2 ± 0.2 μM) (Fig. 4). MP uncaging of Bhc-1400W was performed at the laser exit and on the microscope stage to verify that a similar degree of uncaging could be achieved on the microscope stage as at the laser exit. Furthermore, Bhc-1400W was a very poor inhibitor of nitrite production from LPS-induced RAW 264.7 cells ($IC_{50} > 200$ μM). The inhibitory potency of the protecting group, Bhc, was also assessed. An IC_{50} value of 282 μM demonstrated that Bhc was also a poor inhibitor of nitrite production; UV irradiated Bhc did not inhibit nitrite production from RAW 264.7 cells (Fig. 4). The ratio of the IC_{50} value for Bhc-1400W over the IC_{50} value for 1400W is approximately 100 indicating a potentially broad therapeutic range for the use of Bhc-1400W in cell culture.

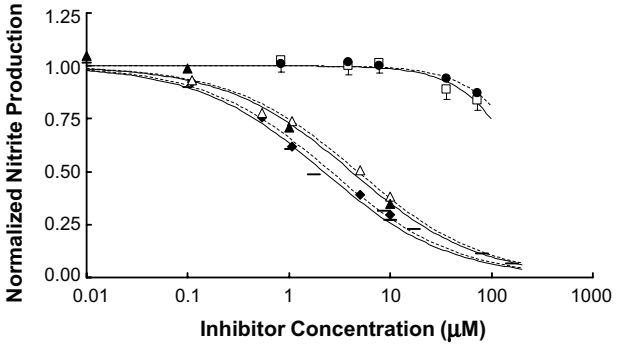

Figure 4. IC_{50} curves of 1400W, UV uncaged Bhc-1400W, MP uncaged Bhc-1400W, Bhc, and Bhc-1400W characterizing the inhibition of nitrite production from activated RAW 264.7 cells. IC_{50} values of 1400W (-,-, 2.2 ± 0.2 μM), UV uncaged Bhc-1400W (◆, --, 2.6 ± 0.1 μM), MP uncaged Bhc-1400W at the laser exit (▲,–, 4.2 ± 0.8 μM), MP uncaged Bhc-1400W on the microscope stage (△,--, 4.8 ± 0.3 μM), Bhc-1400W (□,–, 217 ± 25 μM), and Bhc (●,--, 282 ± 18 μM) characterizing the attenuation of nitrite production from LPS activated RAW 264.7 cells were determined. Nitrite production from RAW 264.7 cells induced to produce ·NO with 1 μg/mL LPS was 22 μM. MP uncaging of Bhc-1400W was not performed in the presence of RAW 264.7 cells. Errors bars indicate 1 standard deviation and are representative of collected data.

2.5. Toxicity analysis

A validated 3-(4,5-dimethylthiazol-2-yl)-2,5-diphenyl tetrazolium bromide (MTT) assay was used to determine the toxicity of 1400W, uncaged Bhc-1400W, Bhc, and Bhc-1400W on RAW 264.7 cells. This viability assay monitors the absorbance of a purple formazan product that is produced by metabolically active cells in the presence of the MTT reagent.[33–35] As healthy and viable cells are metabolically active, they will produce more formazan product giving a higher absorbance reading than stressed, or unhealthy cells. Compounds were incubated with RAW 264.7 cells for 36 h. The CD_{50} value (i.e., the compound concentration that effects a 50% reduction in cellular activity) of 1400W was 6.7 ± 1 mM, indicating that it is not toxic to RAW 264.7 cells at the concentrations of less than 10 μM used to inhibit nitrite production (Fig. 5). The photolabile caged inhibitor, Bhc-1400W, was not toxic to the RAW 264.7 cells even at a concentration of 1 mM. The CD_{50} value for UV photoactivated Bhc-1400W and Bhc were 700 ± 100 μM and 700 ± 200 μM, respectively.

The cellular toxicity level (mg of drug/10^3 cells) for UV uncaged Bhc-1400W is three orders of magnitude larger than the dose required to effectively inhibit nitrite production from LPS-induced RAW 264.7 cells (Fig. 5). These results are in good agreement with a previous toxicity study performed with the murine adrenal medulla PC-12 cell line and the erythrosine B exclusion assay where the calculated CD_{50} values for 1400W and Bhc-1400W were estimated to be approximately 1 mM for both species.[24] Furthermore, no toxicity was observed following exposure of RAW 264.7 cells cultured in 25 μL of cell media containing Bhc-1400W to MPLSM. MPLSM was performed using a 10× objective at an average power of 110 mW for 7 h. The focal volume was focused 250 μm above the cell monolayer.

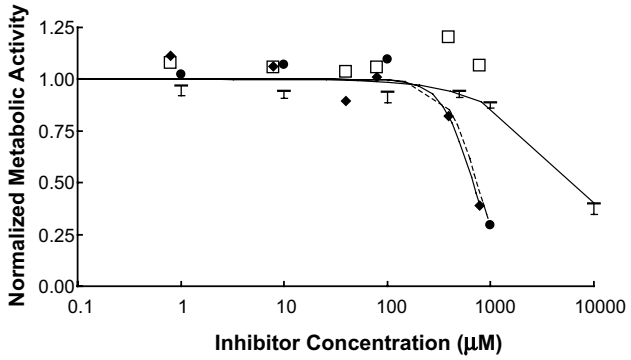

Figure 5. Toxicity of 1400W, UV uncaged Bhc-1400W, and Bhc-1400W to macrophage RAW 264.7 cells. The toxicity of 1400W (-,-, 6,742 ± 916 μM), UV uncaged Bhc-1400W (◆,--, 673 ± 138 μM), Bhc (●,–, 738 ± 198 μM), and Bhc-1400W (□, not determined) to murine macrophage RAW 264.7 cells were determined. CD_{50} values for 1400W, UV uncaged Bhc-1400W, and Bhc are given in parentheses. Errors bars indicate 1 standard deviation and are representative of collected data.

2.6. Drug photoactivation in the presence of cells

The ultimate test of this methodology was to photoactivate the caged inhibitor in the presence of live cells. 30,000 RAW 264.7 cells were cultured in 25 μL of cell media in a 384-well plate containing 1 μg/mL LPS and either 10 μM 1400W, 10 μM UV uncaged Bhc-1400W, or 60 μM of Bhc-1400W. A mode-locked 750 nm NIR laser beam was focused through a 10 × objective 250 μm above one of the wells containing Bhc-1400W for 1.5 h. The power exiting the 10 × objective was between 80 and 90 mW for three independently performed experiments. Based on multiphoton theory[36] and the data shown in Figure 4, exposure of a well containing Bhc-1400W to MPSLM was expected to produce a significant decrease in nitrite production. The data shown in Figure 6 indicates that the system behaves as expected. Exposure of cells to 60 μM of Bhc-1400W resulted in a 20% reduction in nitrite production, but following MPLSM, LPS-stimulated nitrite production in these wells was abolished. The MTT assay confirmed that the metabolic activity of cells exposed to 1400W, Bhc-1400W, uncaged Bhc-1400W, or MPLSM was not significantly different from control wells. These results are in agreement with the toxicity analysis presented above. To our knowledge, this is the first demonstration of a bulk therapeutic effect (i.e., reduction in ·NO production) via multiphoton photoactivation of a caged drug performed in cell culture.

3. Discussion

The potent inhibitor 1400W is highly selective for iNOS over eNOS and nNOS, as determined by kinetic studies with purified enzyme,[22,24] and in tissue and animal models of septic shock and ischemia.[22,37] Kinetic studies showed 1400W to be a slow, tight-binding inhibitor of iNOS, and a poor, classically-competitive inhibitor of eNOS and nNOS.[22] Although 1400W is toxic at high concentrations (intravenous bolus dose of 50 mg/kg) it has been used effectively at much lower, therapeutic concentrations in cell culture, tissue slices, and animal models to inhibit the cytotoxic production of ·NO from iNOS.[22,37] 1400W decreases the invasiveness of the human colorectal adenocarcinoma HRT-18 cell line when administered at a concentration of 500 μM.[2] Perfusion of rat aortic rings with 1400W significantly decreased iNOS activity, but not eNOS activity confirming selectivity of 1400W in tissue slices.[22] Animal models of septic shock, cerebral ischemia, and cancer showed the beneficial affects of iNOS inhibition by 1400W.[22,37,38]

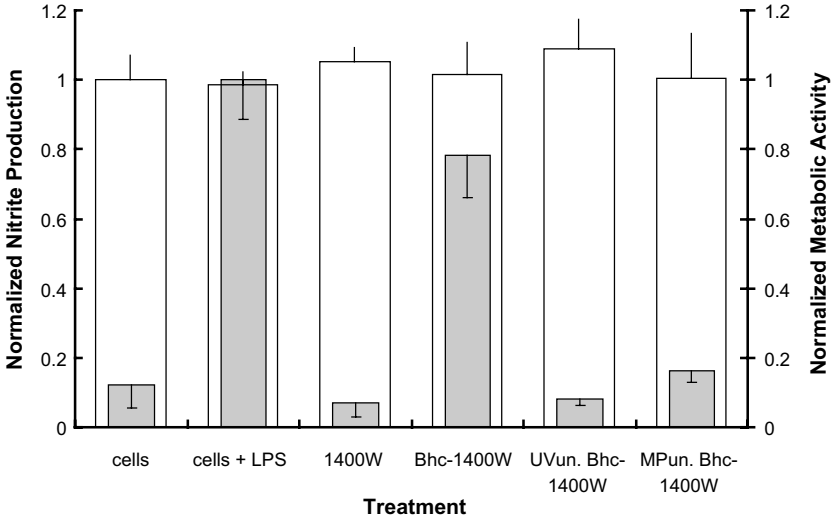

Figure 6. Photoactivation of Bhc-1400W in the presence of RAW 264.7 cells. Normalized nitrite production (dark bars, left-hand scale) and normalized metabolic activity (light bars, right-hand scale) for 30,000 RAW 264.7 cells cultured in 25 μL of cell culture media containing no LPS (cells), or 1 μg/mL LPS (cells + LPS) plus 10 μM 1400W (1400W), 60 μM Bhc-1400W (Bhc-1400W), 10 μM UV uncaged Bhc-1400W (UVun. Bhc-1400W), or 60 μM (MPun. Bhc-1400W) are shown. Total nitrite production from control wells of cells with LPS was 16 μM. Error bars denote the standard deviations of three independently performed experiments.

As well, the septic shock and cerebral ischemia models showed no significant inhibition of nNOS activity.[22,37] The high potency and solubility of 1400W, coupled with its low toxicity, make it an ideal pro-drug for studies aimed at demonstrating controlled photorelease of 1400W from a photolabile-protecting group.

The ratios of the IC_{50} value of caged Bhc-1400W over 1400W calculated in the presence of iNOS enzyme and in RAW 264.7 cell culture are 19 and 100, respectively, indicating that a broader therapeutic range exists in cell culture. It is likely that the improved therapeutic range is achieved because Bhc-1400W is not cell permeable, or is much less permeable, than 1400W. Bhc-glutamate, originally synthesized by Furuta et al. (1999), was not transported into cells, or exhibited very poor cellular uptake. In contrast, uptake of 1400W by RAW 264.7 cells is rapid. A previous report has also commented on the reduction in inhibitory potency that occurs in cell culture due to limited cellular uptake of NOS inhibitors.[39,40] In this study, poor cellular uptake is more pronounced for Bhc-1400W than 1400W. Therefore, conjugation of an appropriate caging molecule to a drug may reduce the efficacy of the caged drug by inhibiting both cellular uptake and binding of the drug to its target. This advantage should motivate the re-examination of previously synthesized candidate drugs that exhibited good efficacy but unacceptable toxicity. For drugs whose toxicity is a result of nonspecific cellular uptake, as opposed to toxicity arising from drug clearance, systemic caged pro-drug delivery should be possible without inducing toxic side effects in nontarget tissues.

A second significant benefit of low cellular uptake of Bhc-1400W is that MP uncaging occurs extracellularly. Although MPLSM is not as destructive to cells and tissues as standard confocal microscopy, there exists an upper threshold to the dose of MPLSM that cells can tolerate.[41] Interestingly, all reports focusing on the cytotoxic effects of MPLSM have been concerned with imaging protocols where the multiphoton focal volume is rastered intracellularly.[41,42] The cytotoxic effects of imaging parameters such as laser pulse width[43] and mean power[44] have been examined. At power levels less than 10 mW with high numerical aperture optics, NIR induced photodamage is postulated to occur due to two-photon absorption by endogenous intracellular absorbers such as NAD(P)H and porphyrins, that lead to the production of reactive oxygen species and subsequent indirect DNA damage.[41] These cytotoxic effects will be less pronounced when a caged therapeutic is activated extracellularly. In this study, the laser focal point was positioned 250 μm above the RAW 264.7 cell monolayer. Using image guided focal volume positioning it should be possible to establish uncaging in vessels and capillaries in and upstream of target tissues. For the MP uncaging protocols used, the theoretical axial characteristic length of the MP excitation volume is expected to vary between 22 and about 100 μm for ellipsoidal Gaussian and Gaussian–Lorenzian spatial laser intensity distributions,[36] respectively. Therefore, minimal two-photon excitation should occur within cells and no decrease in cell viability should be observed. This hypothesis is in agreement with experimental results.

A critical factor in designing caged therapeutics is the extent to which conjugation of a caging molecule to a drug masks the drug's biological activity. For Bhc-1400W, a first generation caged therapeutic, the biological activity is decreased at least 100-fold. This significant decrease has been achieved despite the fact the amidine moiety of 1400W[22] that is responsible for this molecule's tight binding inhibition with iNOS was not directly conjugated to Bhc.[24] With this broad activation range, uncaging 10 μL of a concentrated Bhc-1400W solution is equivalent to releasing approximately 1 mL of a therapeutic concentration of 1400W directly into the tissue. If the biological activity of caged therapeutics can be reduced even further, then several mL equivalents of active drug may be released at the desired site in situ using a single laser beam. Multiple focal volumes, using single mode fiber optic delivery, might be used to release a drug in larger tissue regions.

A relatively new MP cage, 8-bromo-7-hydroxyquinoline (BHQ), has been synthesized.[45] Although the two-photon action uncaging cross section for this molecule is ca. 82% of that for Bhc at 740 nm, and it is not as stable in the dark as Bhc, it exhibits a higher solubility in aqueous solutions than Bhc.[45] Synthesis of BHQ-1400W and an evaluation of this molecule as a caged therapeutic in comparison to Bhc-1400W would be of interest. A second molecule that may be synthesized for this purpose would be Bhc^2-1400W. Synthesis of this molecule would involve coupling Bhc to both the amine and amidine functional groups of 1400W. Synthesis of a Bhc-1400W like molecule with Bhc conjugated to amidine moiety of 1400W is difficult. Therefore, Bhc was conjugated to the amine moiety of 1400W, giving Bhc-1400W. Synthesis of Bhc^2-1400W appears to be the simplest method of inactivating the amidine moiety of 1400W using Bhc-like caging molecules.

Uncaging biologically relevant molecules by multiphoton excitation provides significant advantages in comparison to single photon excitation. In MPLSM, a mode locked, femtosecond pulsed, near infrared laser is typically used to excite a fluorophore or photorelease a caged compound by the near simultaneous absorption of multiple photons.[20,23,46] Excitation or uncaging is intrinsically confined to the vicinity of the focal point of the objective lens due to the requirement for near simultaneous absorption of multiple photons. Using high numerical aperture optics, the two-photon volume of excitation is approximately $0.1\,\mu m^3$, allowing for spatially controlled release of caged molecules. MPLSM also confers the advantages of improved tissue penetration depths and reduced tissue photodamage as NIR wavelengths are used as opposed to UV–vis sources.[20,23,41] Tissue penetration depths up to 1 mm have been achieved using MPLSM.[47,48] Significantly, the out of focus NIR light generated by MPLSM harmlessly passes through cells and tissues as most biological molecules do not absorb light in this spectral range.[41] It is the combination of these factors that permits the use

of MPLSM for spatial and temporal control of drug photoactivation within tissues.

Future work will involve examining the effects of the scattering properties of biological tissue on the efficacy of MP uncaging of Bhc-1400W, the use of several single mode optical fibers to focus several focal volumes onto a sample simultaneously, the in vivo pharmacokinetic distribution of caged and uncaged drug, and the effects of various MP uncaging protocols on in vivo cellular viability. The required power to be delivered in vivo will depend on several factors including the photosensitivity of the target tissue, the required active drug concentration, the reduction in biological activity that results from caging the drug, the permitted uncaging time, the number of focal volumes applied, the local tissue pharmacokinetics, and the efficiency of the uncaging process within the target tissue. Although much lower laser powers may be required to perform in vivo experiments, the intensity at the laser focal point of the experiments performed in cell culture in this report are of similar intensity as those used to perform long term MPLSM imaging. In the uncaging experiments presented, higher laser powers were used in conjunction with low numerical apertures. In long term MPLSM imaging low laser powers are used in combination with high numerical apertures.[36] Furthermore, as mentioned previously, uncaging a compound extracellularly will reduce phototoxicity.

In summary, Bhc-1400W exhibits a broad therapeutic range over which photocontrol of ·NO production may be achieved in mammalian cell culture. This report provides the first instance of MP photoactivation of a caged drug resulting in a bulk therapeutic affect. This technology offers the possibility of spatial and temporal control drug activity, the lack of which is one of the major problems currently associated with systemic drug administration.

4. Experimental

4.1. Materials

Unless noted otherwise, all reagents were purchased from Sigma–Aldrich Canada, Ltd (Oakville, ON, Canada) and used without further purification.

4.2. Preparation of 1400W and Bhc-1400W

The compounds 1400W and Bhc-1400W were prepared using a modification of the procedure previously described.[24] For the synthesis of Bhc-1400W, only acetonitrile was used as solvent. After concentration of the crude reaction mixture, the material was suspended in 20:80 acetonitrile–water (0.1% trifluoroacetic acid (TFA)) with vigorous stirring, and then filtered through a plug of glass wool. Purification was performed by HPLC and characterized by Z-spray mass spectrometry using positive ionization mode.

The Bhc-1400W conjugate was purified by HPLC using a Zorbax ODS C18 Semi-Prep column (9.4 × 250 mm, 5 mm). The sample was loaded in 20–25% CH_3CN in H_2O (0.1% TFA in both solvents). The flow rate was 4 mL/min, and a gradient mobile phase was employed (CH_3CN–H_2O 20:80 up to 40:60 over 35 min). Absorbance was observed at 260 and 320 nm, and the broadly eluting fraction between 20 and 28 min was collected, and then lyophilized to provide a fluffy solid. A Novapak C18 Analytical column (3.9 × 150 mm) was used to analyze the final product. The flow rate was 1 mL/min, and a gradient mobile phase was employed (CH_3CN–H_2O (0.1% TFA) 5:95 up to 95:5 over 35 min). Absorbance was observed at 260 and 320 nm, and Bhc-1400W eluted as a sharp peak at 15.2 min.

4.3. Protein expression and purification

Human iNOS enzyme carrying a deletion of the first 70 amino acids and an amino terminal polyhistidine tail was co-expressed with CaM in *E. coli* and purified using metal chelating chromatography followed by 2′,5′-ADP column chromatography.[24,49]

4.4. Enzyme kinetics

The activity of iNOS was determined using the oxyhemoglobin capture assay[50,51] that yields results consistent with the direct radioactive assay that monitors the formation of L-[^3H]-citrulline from L-[^3H]-arginine.[52] Enzyme kinetic experiments were performed on a 96-well plate reader (Spectramax 190, Molecular Devices, Sunnyvale, CA, USA). The plate reader was controlled using SOFTMAX PRO software Version 3.0 (Molecular Devices, Sunnyvale, CA, USA). Nitric oxide-mediated oxidation of HbO_2 was monitored at 401 nm ($\Delta\varepsilon_{401\,nm(metHb–HbO_2)}$ of 0.101 ± 0.005 $OD_{401\,nm}$/nmol). Quadruplicate reactions were initiated by the addition of L-arginine and monitored on the 96-well plate reader at 30 °C. For the determination of IC_{50} values, 100 μL reaction mixtures contained 50 mM Tris–HCl (pH 7.5 at room temperature), 1% (v/v) glycerol, 500 μM NADPH, 5 μM (6*R*)-5,6,7,8-tetrahydrobiopterin (H_4B), 1 μM CaM, 1 mM $CaCl_2$, 16 μM dithiothreitol (DTT), 1 μM FAD, 1 μM FMN, 100 units/mL superoxide dismutase (SOD), 50 units/mL catalase, 10 μM bovine HbO_2, 0.2 mg/mL bovine serum albumin, 25 μM L-arginine and 30 nM iNOS (k_{cat} ca. 405 ± 16 nmol ·NO min^{-1} mg $iNOS^{-1}$, K_m (L-arg) equal to 4.5 ± 0.6 μM). Enzyme in the presence or absence of varying amounts of 1400W, Bhc-1400W, or uncaged Bhc-1400W, and in the presence of 500 μM NADPH, 10 μM FAD, 10 μM FMN, 50 μM H_4B, 160 μM DTT, 100 units/mL SOD, and 50 units/mL catalase were incubated at 30 °C for 15 min. For these experiments the Bhc-1400W was exposed to UV light for 15 min or to MP irradiation for between 0.5 and 4 h to obtain the uncaged samples.

4.5. Uncaging of Bhc-1400W

Bhc-1400W was solubilized by vigorous agitation for 0.5–1 h at 4 °C in the dark, and solutions were sterilized using a 0.22 μm syringe filter. Typical Bhc-1400W concentrations, determined by UV–vis spectrophotometry ($\lambda_{max} = 368$ nm, $\varepsilon = 17{,}470\ M^{-1}cm^{-1}$), varied

from 600 μM to 1.2 mM in 100 mM KCl/10 mM Mops buffer (pH 7.2) (KMops) and cell culture media, respectively.[24] UV uncaging of Bhc-1400W was performed at 366 nm using a hand held UV lamp (model UVGL-15, Ultra-Violet Products, Upland, CA, USA). Bhc-1400W was uncaged for 15 min.

MP uncaging of Bhc-1400W on the microscope stage was performed on a system consisting of a titanium:sapphire (Ti:Sa) laser (Mira Model 900-B, Coherent Inc., Santa Clara, CA, USA) pumped by a neodymium:yttrium aluminum garnet (Nd:YAG) laser (Verdi, Coherent Inc., Santa Clara, CA, USA), a Pockels cell (model 350-50, Conoptics, Danbury, CT, USA), a 3× beam expander (model T81-3×, Newport Instruments Canada Ltd, Mississauga, ON, Canada), a scan head (MRC-600, Bio-Rad Microscience Ltd, Mississauga, ON, Canada), an inverted microscope (Axiovert S100TV, Carl Zeiss Canada Ltd, Toronto, ON, Canada), an objective lens (A-Plan 10×/0.25 Ph 1; Carl Zeiss Canada Ltd, Toronto, ON, Canada), and external mirrors.

Multiphoton uncaging at the exit aperture of the mode locked (76 MHz repetition rate, ca. 200 fs pulse width) Ti:Sa laser was performed by placing a quartz cuvette in the focal plane of the objective lens. A 25 μL aliquot of concentrated Bhc-1400W (ca. 1 mM) dissolved in cell culture media was MP uncaged for 6 h (MP uncaged Bhc-1400W at the laser exit (Fig. 4)). Uncaging was performed at 740 nm.[23] The laser power exiting the cuvette was 200 mW. Dark uncaging of Bhc-1400W was monitored with a sample kept at room temperature beside the cuvette.

Multiphoton uncaging on the microscope stage was performed at 750 nm. The power exiting the 10× objective was between 100 and 110 mW and the laser was focused 50 μm above the coverglass of a microcuvette. Uncaging was performed in 10 μL of 250 μM Bhc-1400W dissolved in KMops, at a zoom of 1 under slow scan (ca. 7 μs dwell time per 1.8 × 1.8 μm pixel, scan area 1387 μm by 925 μm) or using a parked laser beam for 0.5–4 h (Fig. 1). Uncaging was also performed in 20 μL of 600 μM Bhc-1400W dissolved in cell culture media, at a zoom of 2 under slow scan (ca. 7 μs dwell time per 0.9 × 0.9 μm pixel, scan area 694 μm by 462 μm) for 7.5 h (MP uncaged Bhc-1400W on the microscope stage (Fig. 4)).

MP uncaging in the presence of RAW 264.7 cells was performed on the microscope stage at 750 nm under at a zoom of 1 under slow scan. The power exiting the 10× objective was between 80 and 90 mW. The focal volume was focused 250 μm above a 70% confluent monolayer of RAW 264.7 cells for 1.5 h. RAW 264.7 cells (30,000) were cultured in a 384-well plate with a coverglass bottom (Cat. No 357309, BD Biosciences, Oakville, ON) containing 25 μL of cell culture media, 1 μg/mL LPS, and 60 μM Bhc-1400W. Cells were allowed to adhere to the 384-well plate for one hour prior to MP uncaging. Control wells were also cultured on the 384-well plate. Cells were also exposed to 7 h of MP irradiation to assess laser toxicity. After exposure to the NIR laser beam, cells were placed in an incubator for 24 h and the Griess and MTT assays performed to measure nitrite production and cell viability, respectively.

4.6. Cell passaging

The murine macrophage cell line RAW 264.7 (ATCC TIB 71) was cultured in Dulbecco's modified Eagle's medium (DMEM, low glucose, no phenol red or glutamine) supplemented with 4 mM L-glutamine and 10% (v/v) fetal bovine serum (FBS). All materials were obtained from the Invitrogen Corporation (Burlington, ON, Canada). Cells were maintained at 37 °C in a humidified 5% CO_2/95% air atmosphere. The RAW 264.7 cell doubling time under these conditions was determined to be 22 ± 0.5 h.

4.7. Induction of ·NO production in RAW 264.7 cells

RAW 264.7 cells were seeded at a density of 150,000 cells/well in sterile, tissue culture treated 96-well plates (Corning, NY, USA) by aliquoting 200 mL of a 750,000 cells/mL cell suspension into each well. Twenty four hours later 150 μL of media was removed from each well and 200 μL of a solution containing fresh media, gamma irradiated LPS (final well concentration of 1 μg/mL) (Sigma–Aldrich, Canada Ltd, Oakville, ON, Canada), and inhibitors (final well concentrations of 0.01–100 μM) were added to each well.

4.8. Determination of nitrite concentration

Nitrite concentrations were determined using the Griess assay[27] 24 h after LPS stimulation, unless indicated otherwise. Equal volumes of Griess reagent,[53,54] one part 1% (w/v) sulfanilamide solution in 5% phosphoric acid and one part 0.1% (w/v) N-(-1-napthyl)ethylenediamine in ultra pure water, and cell culture supernatant were combined. The mixtures (200 or 40 μL) were incubated for 9 min prior to 1 min of mixing on a 96-well plate reader (Spectramax 190, Molecular Devices, Sunnyvale, CA, USA) or a 384-well plate reader (Multiskan Ascent, Labsystems Inc., Helsinki, Finland), respectively. $OD_{540–630\,nm}$ measurements were obtained, and sodium nitrite standards were used to convert OD readings into nitrite concentrations.

4.9. Determination of cell viability

The viability of RAW 264.7 cells was measured using the MTT assay.[29,34] After removal of supernatant, cells were incubated for four hours in cell culture media containing 450 μg/mL MTT. Formazan crystals were dissolved in DMSO and $OD_{550–690\,nm}$ measurements obtained. The toxicity of 1400W, Bhc-1400W, and uncaged Bhc-1400W was determined by preparing serial dilutions of inhibitors (1 μM–10 μM). Cells (10,000 cells/well, 250 μL media/well) were allowed to incubate with inhibitors for 36 h.

4.10. Regression

IC_{50} versus uncaging time data was fit to the decaying exponential shown below by nonlinear regression (Statistics Toolbox, MATLAB version 6.1, Mathworks, Boston, MA) (Fig. 1, panel B):

$$IC_{50}(t) = (IC_{50}^{Bhc-1400W} - IC_{50}^{UVun}) \exp(-k_{un}^{IC_{50}} t) + IC_{50}^{UVun} \quad (1)$$

where t is the time (h), $IC_{50}^{Bhc-1400W}$ is the IC_{50} value for Bhc-1400W (344 ± 50 nM), IC_{50}^{UVun} is the IC_{50} value for UV uncaged Bhc-1400W (20 ± 3 nM), and $k_{un}^{IC_{50}}$ is the apparent first-order time constant characterizing the conversion of IC_{50} values from $IC_{50}^{Bhc-1400W}$ to IC_{50}^{UVun} during uncaging (h^{-1}).

Normalized responses (normalized iNOS activity (nM ·NO produced·s^{-1}), nitrite production (μM), MTT turnover ($OD_{550-690\,nm}$)) versus inhibitor concentration data were fit to Eq. 2 by nonlinear regression (Statistics Toolbox, MATLAB version 6.1, Mathworks, Boston, MA):

$$\text{Normalized response} = \frac{1}{1 + \left(\frac{[I]}{IC_{50}}\right)^n} \quad (2)$$

where the normalized response is the value of the response at inhibitor concentration I over the response measured in the absence of inhibitor, $[I]$ is the inhibitor concentration (nM), IC_{50} (or CD_{50} for toxicity analysis) is the inhibitor concentration that effects a 50% reduction in the normalized response, and n is the logistic sensitivity.

Acknowledgements

This research was supported by Grants 203286 to E.J. and 183521 to J.G.G. from the Natural Sciences and Engineering Research Council of Canada.

References and notes

1. Stuehr, D. J. *Biochim. Biophys. Acta* **1999**, *1411*, 217.
2. Siegert, A.; Rosenberg, C.; Schmitt, W. D.; Denkert, C.; Hauptmann, S. *Br. J. Cancer* **2002**, *86*, 1310.
3. Vallance, P.; Leiper, J. *Nat. Rev. Drug. Discov.* **2002**, *1*, 939.
4. Albrecht, E. W.; Stegeman, C. A.; Heeringa, P.; Henning, R. H.; van Goor, H. *J. Pathol.* **2003**, *199*, 8.
5. Miranda, K. M.; Espey, M. G.; Jourd'heuil, D.; Grisham, M. B.; Fukuto, J. M.; Feelisch, M.; Wink, D. A. In *Nitric Oxide: Biology and Pathology*; Ignarro, L. J., Ed.; Academic: San Diego, CA, 2000; pp 41–55.
6. Lutz, P. L.; Nilsson, G. E. *Brain without Oxygen: Causes of Failure and Mechanisms for Survival*; Landes Bioscience: New York, 1997.
7. Bogdan, C. *Nat. Immunol.* **2001**, *2*, 907.
8. Kroncke, K. D.; Fehsel, K.; Suschek, C.; Kolb-Bachofen, V. *Int. Immunopharmacol.* **2001**, *1*, 1407.
9. Iadecola, C. *Trends Neurosci.* **1997**, *20*, 132.
10. Yonekura, Y.; Koshiishi, I.; Yamada, K.; Mori, A.; Uchida, S.; Nakamura, T.; Utsumi, H. *Nitric Oxide* **2003**, *8*, 164.
11. Iskit, A. B.; Guc, O. *Acta Pharmacol. Sin.* **2003**, *24*, 953.
12. Hobbs, A. J.; Higgs, A.; Moncada, S. *Annu. Rev. Pharmacol. Toxicol.* **1999**, *39*, 191.
13. Petros, A.; Lamb, G.; Leone, A.; Moncada, S.; Bennett, D.; Vallance, P. *Cardiovasc. Res.* **1994**, *28*, 34.
14. Szabo, C.; Southan, G. J.; Thiemermann, C. *Proc. Natl. Acad. Sci. U.S.A.* **1994**, *91*, 12472.
15. Park, C. S.; Pardhasaradhi, K.; Gianotti, C.; Villegas, E.; Krishna, G. *Biochem. Biophys. Res. Commun.* **1994**, *205*, 85.
16. Park, C.-S.; Park, R.; Gopal, K. *Life Sci.* **1996**, *59*, 219.
17. Guo, F. H.; De Raeve, H. R.; Rice, T. W.; Stuehr, D. J.; Thunnissen, F. B.; Erzurum, S. C. *Proc. Natl. Acad. Sci. U.S.A.* **1995**, *92*, 7809.
18. Cunningham, M. L.; Johnson, J. S.; Giovanazzi, S. M.; Peak, M. *J. Photochem. Photobiol.* **1985**, *42*, 125.
19. Williams, R. M.; Zipfel, W. R.; Webb, W. W. *Curr. Opin. Chem. Biol.* **2001**, *5*, 603.
20. Denk, W.; Strickler, J. H.; Webb, W. W. *Science* **1990**, *248*, 73.
21. Zipfel, W. R.; Williams, R. M.; Webb, W. W. *Nat. Biotechnol.* **2003**, *21*, 1369.
22. Garvey, E. P.; Oplinger, J. A.; Furfine, E. S.; Kiff, R. L.; Laszlo, F.; Whittle, B. J. R.; Knowles, R. G. *J. Biol. Chem.* **1997**, *272*, 4959.
23. Furuta, T.; Wang, S. S.-H.; Dantzker, J. L.; Dore, T. M.; Bybee, W. J.; Callaway, E. M.; Denk, W.; Tsien, R. Y. *Proc. Natl. Acad. Sci. U.S.A.* **1999**, *96*, 1193.
24. Montgomery, H. J.; Perdicakis, B.; Fishlock, D.; Lajoie, G. A.; Jervis, E.; Guillemette, J. G. *Bioorg. Med. Chem.* **2002**, *10*, 1919.
25. Brown, E. B.; Webb, W. W. *Meth. Enzymol.* **1998**, *291*, 356.
26. Lu, M.; Fedoryak, O. D.; Moister, B. R.; Dore, T. M. *Org. Lett.* **2003**, *5*, 2119.
27. Green, L. C.; Wagner, D. A.; Glogowski, J.; Skipper, P. L.; Wishnok, J. S.; Tannenbaum, S. R. *Anal. Biochem.* **1982**, *126*, 131.
28. Chen, B.; Keshive, M.; Deen, W. M. *Biophys. J.* **1998**, *75*, 745.
29. Kiemer, A. K.; Muller, C.; Vollmar, A. M. *Immunol. Cell. Biol.* **2002**, *80*, 550.
30. Chen, Y. C.; Shen, S. C.; Lee, W. R.; Hou, W. C.; Yang, L. L.; Lee, T. J. *J. Cell. Biochem.* **2001**, *82*, 537.
31. Raschke, W. C.; Baird, S.; Ralph, P.; Nakoinz, I. *Cell* **1978**, *15*, 261.
32. Nathan, C. *FASEB J.* **1992**, *6*, 3051.
33. Mosmann, T. *J. Immunol. Methods* **1983**, *65*, 55.
34. van de Loosdrecht, A. A.; Beelen, R. H.; Ossenkoppele, G. J.; Broekhoven, M. G.; Langenhuijsen, M. M. *J. Immunol. Methods* **1994**, *174*, 311.
35. van de Loosdrecht, A. A.; Nennie, E.; Ossenkoppele, G. J.; Beelen, R. H.; Langenhuijsen, M. M. *J. Immunol. Methods* **1991**, *141*, 15.
36. Xu, C.; Webb, W. W. In *Multiphoton Excitation of Molecular Fluorophores and Nonlinear Laser Microscopy*; Lakowicz, J. R., Ed.; Plenum: New York, 1997; Vol. 5, pp 471–540.
37. Parmentier, S.; Bohme, G. A.; Lerouet, D.; Damour, D.; Stutzmann, J.-M.; Margail, Isabelle; Plotkine, M. *Br. J. Pharmacol.* **1999**, *127*, 546.
38. Thomsen, L. L.; Scott, J. M.; Topley, P.; Knowles, R. G.; Keerie, A. J.; Frend, A. J. *Cancer Res.* **1997**, *57*, 3300.
39. Schmidt, K.; Klatt, P.; Mayer, B. *Biochem. J.* **1994**, *301*, 313.

40. Schmidt, K.; List, B. M.; Klatt, P.; Mayer, B. *J. Neurochem.* **1995**, *64*, 1469.
41. Konig, K. *J. Microsc.* **2000**, *200*, 83.
42. Tirlapur, U. K.; Konig, K.; Peuckert, C.; Krieg, R.; Halbhuber, K. J. *Exp. Cell Res.* **2001**, *263*, 88.
43. Konig, K.; Becker, T. W.; Fischer, P.; Riemann, I.; Halbhuber, K.-J. *Opt. Lett.* **1999**, *24*, 113.
44. Konig, K.; So, P. T. C.; Mantulin, W. W.; Gratton, E. *Opt. Lett.* **1997**, *22*, 135136.
45. Fedoryak, O. D.; Dore, T. M. *Org. Lett.* **2002**, *4*, 3419.
46. Denk, W. *Proc. Natl. Acad. Sci. U.S.A.* **1994**, *91*, 6629.
47. So, P. T.; Dong, C. Y.; Masters, B. R.; Berland, K. M. *Annu. Rev. Biomed. Eng.* **2000**, *2*, 399.
48. Theer, P.; Hasan, M. T.; Denk, W. *Opt. Lett.* **2003**, *28*, 1022.
49. Ghosh, D. K.; Rashid, M. B.; Crane, B.; Taskar, V.; Mast, M.; Misukonis, M. A.; Weinberg, J. B.; Eissa, N. T. *Proc. Natl. Acad. Sci. U.S.A.* **2001**, *98*, 10392.
50. Hevel, J. M.; Marletta, M. A. *Methods Enzymol.* **1994**, *233*, 250.
51. Gross, S. S. *Methods Enzymol.* **1996**, *268*, 159.
52. Montgomery, H. J.; Romanov, V.; Guillemette, J. G. *J. Biol. Chem.* **2000**, *275*, 5052.
53. Griess, J. P. *Philos. Trans. R. Soc. Lond.* **1864**, *154*, 667.
54. Griess, J. P. *Ber. Deutsch. Chem. Ges.* **1879**, *12*, 426.